Journal of Biomechanics xxx (2018) xxx–xxx

Contents lists available at ScienceDirect

Journal of Biomechanics

journal homepage: www.elsevier.com/locate/jbiomech
www.JBiomech.com

The relationship of whole human vertebral body creep to geometric, microstructural, and material properties

Daniel Oravec [a], Woong Kim [a], Michael J. Flynn [b], Yener N. Yeni [a,*]

[a] Bone and Joint Center, Henry Ford Hospital, Detroit, MI, United States
[b] Department of Radiology, Henry Ford Hospital, Detroit, MI, United States

ARTICLE INFO

Article history:
Accepted 9 March 2018
Available online xxxx

Keywords:
Creep
Vertebral body
Material properties
Geometry
Microstructure

ABSTRACT

Creep, the time dependent deformation of a structure under load, is an important viscoelastic property of bone and may play a role in the development of permanent deformity of the vertebrae *in vivo* leading to clinically observable spinal fractures. To date, creep properties and their relationship to geometric, microstructural, and material properties have not been described in isolated human vertebral bodies. In this study, a range of image-based measures of vertebral bone geometry, bone mass, microarchitecture and mineralization were examined in multiple regression models in an effort to understand their contribution to creep behavior. Several variables, such as measures of mineralization heterogeneity, average bone density, and connectivity density persistently appeared as significant effects in multiple regression models (adjusted r^2: 0.17–0.56). Although further work is needed to identify additional tissue properties to fully describe the portion of variability not explained by these models, these data are expected to help understand mechanisms underlying creep and improve prediction of vertebral deformities that eventually progress to a clinically observable fracture.

1. Introduction

Creep, the time-dependent deformation of a structure under prolonged load, is understood to play an important role in deformity of vertebral bone due to progressive accumulation of residual strain (Pollintine et al., 2009). To date, aspects of creep have been studied in animal trabecular bone (Bowman et al., 1998, 1994; Manda et al., 2016; Rimnac et al., 1993; Shepherd et al., 2011; Xie et al., 2017), animal vertebrae and motion segments (Bailey et al., 2014; Kim et al., 2012; van der Veen et al., 2008), and demineralized bone (Bowman et al., 1999; Summitt and Reisinger, 2003). Creep properties have also been studied in isolated human cancellous (Kim et al., 2011; Novitskaya et al., 2014; Yamamoto et al., 2006; Zilch et al., 1980) and cortical bone (Caler and Carter, 1989; Fondrk et al., 1988), and vertebral motion segments (Busscher et al., 2011; Kazarian, 1975; Keller et al., 1987; Luo et al., 2012; Pollintine et al., 2009). It has been shown that creep behavior is sensitive to mechanical damage to the bone (Fondrk et al., 1988), disc health (Adams et al., 2006) and is suggested to play a role in fracture healing (Goodship et al., 1998). It has also been suggested that permanent deformation resulting from creep may develop at physiological load levels and contribute to the fatigue behavior of vertebral bone (Yamamoto et al., 2006), resulting in progressive loss of strength and ultimate failure of the bone tissue (Bowman et al., 1998, 1994).

Despite the importance of creep in bone, no previous study has specifically examined creep behavior and addressed the relationship between microstructural organization and creep in human vertebral bodies. Engineering theories suggest that the viscoelastic behavior of cellular materials such as cancellous bone is affected by the distribution of material densities and voids (Ajdari et al., 2009; Andrews and Gibson, 2001; Huang and Gibson, 2003). Correspondingly, previous studies demonstrated that creep is associated with microstructural properties in human and bovine cancellous bone (Kim et al., 2011; Manda et al., 2016). In addition, significant relationships have been demonstrated between uniaxial compressive creep rate and both average and variability of grey values within the bone phase of segmented μCT images (a measure of bone tissue mineralization), in human vertebral cancellous cores (Kim et al., 2011). However, no such relationship was found between bone tissue mineralization and nanoindentation creep rate in femoral cortical bone (Wu et al., 2012).

With results varying between anatomical site, species, and outcomes from different measurement methods, the extent to which

* Corresponding author at: Henry Ford Hospital, Integrative Biosciences Center (iBio), 6135 Woodward, Detroit, MI 48202, United States.
E-mail address: yeni@bjc.hfh.edu (Y.N. Yeni).

https://doi.org/10.1016/j.jbiomech.2018.03.021
0021-9290/

the abovementioned findings can be directly applied to isolated human vertebrae remains unknown. Therefore, the current study aims to establish relationships between creep of human cadaveric vertebral bodies and clinically available measures of vertebral geometry and bone mineral density as well as microstructural and hard tissue properties measured using microcomputed tomography.

2. Methods

Human cadaveric thoraco-lumbar spines were acquired from tissue banks under local IRB approval and T12 vertebrae were harvested from 23 donors. Donors with a history of HIV, hepatitis, diabetes, renal failure, metastatic cancer, osteomalacia, hyperparathyroidism, Paget's disease of bone, spine surgery, cause of death involving trauma, and corticosteroid, anticonvulsant or bisphosphonate use were not included. Vertebral bodies were dissected, soft tissue and posterior elements were removed, and specimens were stored wrapped in saline-soaked gauze at −20 °C until imaging and testing were performed. The donor set consisted of 13 men and 10 women between the ages of 41 and 97.

The prepared specimens were scanned using a custom-built μCT system and reconstructed at an isotropic voxel size of 40 μm (Kim et al., 2015). Specimens were wrapped in saline-soaked gauze throughout scanning to maintain hydration. The largest possible cubical volume of interest (VOI) consisting of only cancellous bone was cropped from the center of the reconstructed bone volume and the VOI was segmented using global thresholding within Microview (GE Healthcare, Illinois, USA). Grey values were preserved during segmentation for calculation of average (μCT.GV.Av), standard deviation (μCT.GV.SD) and coefficient of variation (μCT.GV.CV = μCT.GV.SD/μCT.GV.Av) of grey values as mineralization parameters (Fig. 1). Scan-to-scan consistency was assured by normalizing grey values using a material density phantom present in each scan. Images were then binarized and processed using CT-Analyzer (v1.12.0.0; Bruker, Kontich, Belgium) to obtain 3D measures of bone volume fraction (BV/TV), trabecular thickness (Tb.Th), trabecular number (Tb.N), trabecular spacing (Tb.Sp), degree of anisotropy (DA), connectivity density (Conn.Dn), and structure model index (SMI). Standard deviation (SD) of BV/TV (BV/TV.SD), Tb.Th (Tb.Th.SD), Tb.N (Tb.N.SD) and Tb.Sp (Tb.Sp.SD) were calculated as measures of microstructural heterogeneity from the distribution of 2D stereology results from axial slices, indicating a slice to slice variation of the corresponding variable in the superior-inferior direction (Yeni et al., 2011).

In order to measure volumetric BMD, the same specimens were scanned using high resolution computed tomography (HRCT) and reconstructed at 0.7 mm axial pixel spacing with 0.75 mm slice thickness (Siemens Sensation 64). The vertebrae were mounted and consistently aligned via a custom, radiolucent clamping tray in the center of a scanning tank filled with 0.9% saline to simulate surrounding soft tissue. A single, unique threshold value that delineates bone from soft tissue was determined for each vertebral body and applied within a custom segmentation algorithm to produce a closed surface grey value mask of the vertebral body (Zauel et al., 2005). Volume masks representing cancellous and cortical bone were prepared from HRCT images using a previously described semi-automatic segmentation method (Buie et al., 2007; Oravec et al., 2015). The segmented volume masks were multiplied with the original grey value images, from which integral cancellous+cortical (iBMD), volumetric cancellous (cBMD), and shell (shBMD) bone mineral density (BMD) were calculated (Fig. 2a). Integral cancellous+cortical volume (CT-Vol), area of anterior-posterior (AP) and lateral-medial (LM) projections (Area.AP, Area.LM), height and width in AP (Height.AP, Width.AP) and LM (Height.LM, Width.LM) were also recorded using the prepared binary masks (Fig. 2b).

The vertebral bodies were then scanned using dual X-ray absorptiometry (DXA) in AP and LM orientations using a fast array lumbar spine protocol (Hologic Discovery-A). Specimens were again aligned to imaging axes using a radiolucent tray immersed in 0.9% saline. BMD and bone mineral content (BMC) were measured for two views of each vertebra (BMD.AP, BMC.AP, BMD.LM, BMC.LM) within Hologic Discovery software using standard clinical analysis techniques. Area in AP (DXA-Area.AP) and LM (DXA-Area.LM) directions were also recorded.

Following imaging studies, creep tests were conducted in a materials test machine (Model 8850; Instron, Canton, MA) with specimens fully submerged in saline at 37 °C. Vertebral endplates were left intact (i.e., not cut) and potted using a parallel plate jig using dental stone to ensure flat and parallel boundary conditions.

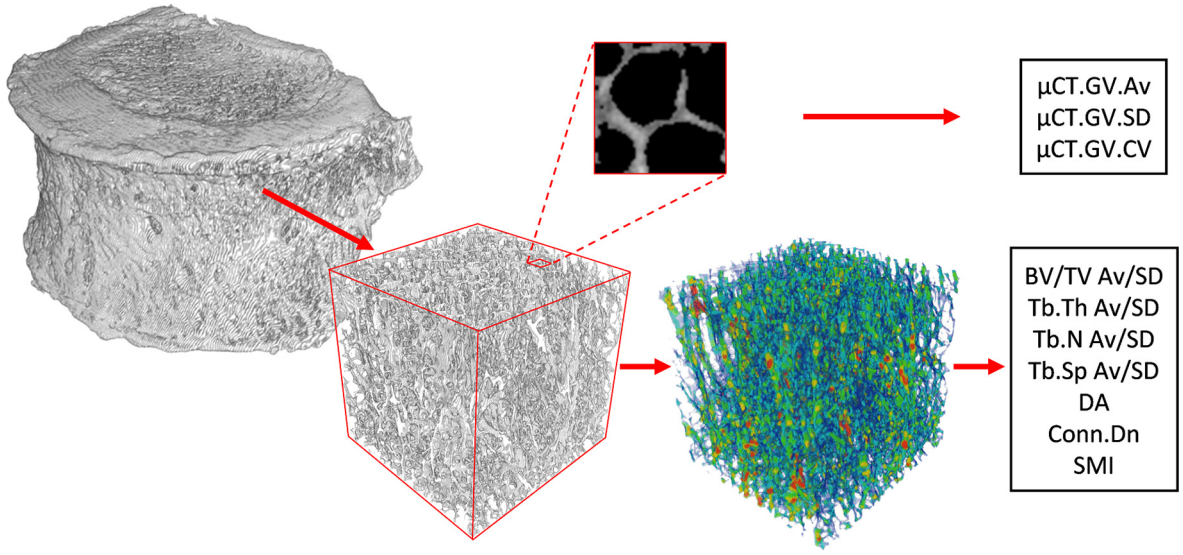

Fig. 1. Cubic volumes of interest were extracted from the cancellous centrum of microcomputed tomography images to calculate stereological parameters (bottom; trabecular thickness map presented). Average, standard deviation, and coefficient of variation of the grey values were calculated using the entire cube (top; exploded 2 mm axial view demonstrating trabecular bone grey value distribution).

Please cite this article in press as: Oravec, D., et al. The relationship of whole human vertebral body creep to geometric, microstructural, and material properties. J. Biomech. (2018), https://doi.org/10.1016/j.jbiomech.2018.03.021